

Optical and infrared photometry of new very low-mass stars and brown dwarfs in the σ Orionis cluster

V. J. S. BÉJAR¹, M. R. ZAPATERO OSORIO², AND R. REBOLO^{1,3}

¹ Instituto de Astrofísica de Canarias, E-38205 La Laguna, Tenerife, Spain

² LAEFF-INTA, P.O. Box 50727, E-28080 Madrid, Spain

³ Consejo Superior de Investigaciones Científicas, Madrid, Spain

Received date will be inserted by the editor; accepted date will be inserted by the editor

Abstract. We present an RI photometric survey covering an area of 430 arcmin² around the multiple star σ Orionis. The observations were conducted with the 0.8 m IAC-80 Telescope at the Teide Observatory. The survey limiting R and I magnitudes are 22.5 and 21, and completeness magnitudes 21 and 20, respectively. We have selected 53 candidates from the I vs. $R-I$ colour-magnitude diagram ($I = 14-20$) that follow the previously known photometric sequence of the cluster. Adopting an age of 2–4 Myr for the cluster, we find that these objects span a mass range from 0.35 M_{\odot} to 0.015 M_{\odot} . We have performed J -band photometry of 52 candidates and K_s photometry for 12 of them, with the result that 50 follow the expected infrared sequence for the cluster, thus confirming with great confidence that the majority of the candidates are bona fide members. JHK_s photometry from the Two Micron All Sky Survey (2MASS) is available for 50 of the candidates and are in good agreement with our data. Out of 48 candidates, which have photometric accuracies better than 0.1 mag in all bands, only three appear to show near-infrared excesses.

Key words: Stars: low-mass, brown dwarfs – Stars: luminosity function, mass function – Stars: colour–magnitude diagrams (H-R diagrams) – Stars: formation – Stars: Open clusters and associations – Stars: individual (σ Orionis)

1. Introduction

The Orion complex, because of its relative closeness and youth, is one of the most suitable sites for understanding low-mass star formation processes. Recently, *ROSAT* pointed observations within this complex has led to the discovery of the very young stellar cluster σ Orionis, around the multiple star of the same name (Walter et al. 1997; Wolk & Walter 1998). Follow-up photometric and spectroscopic studies have revealed a sequence of objects in the colour–magnitude diagram that extends well below the substellar limit (Béjar et al. 1999, hereafter BZOR; Béjar et al. 2001, hereafter BMZO). Studies of the depletion of lithium in the atmosphere of K6–M8.5 type low-mass members of the cluster impose an upper limit of 8 Myr on the age and suggest a most likely cluster age in the interval 2–4 Myr (Zapatero Osorio et al. 2002). *Hipparcos* provides a distance modulus of $m - M = 7.7 \pm 0.7$ (Perryman et al. 1997) for the central star, σ Orionis. This star is affected by a low extinction value of $E(B - V) = 0.05$

(Lee 1968), and the associated cluster also seems to exhibit very little reddening (see BMZO and Oliveira et al. 2002). These combined characteristics of youth, proximity and low extinction make σ Orionis one of the most interesting clusters for studying young substellar objects and the substellar mass function.

In this paper we present an extension of the RI survey conducted by BZOR, with the aim of detecting new low-mass star and brown dwarf candidates in the σ Orionis cluster. We also present near-infrared data for these objects. Details of the observations are indicated in Section 2. In sections 3.1 and 3.2 we explain the selection of the candidates and discuss their membership and the presence of near-infrared excesses. Our conclusions are given in section 4.

2. Observations

2.1. Optical Photometry

We obtained RI images with the IAC-80 Telescope, at the Teide Observatory on 1998 January 22 and 23. The camera

Correspondence to: vbejar@ll.iac.es

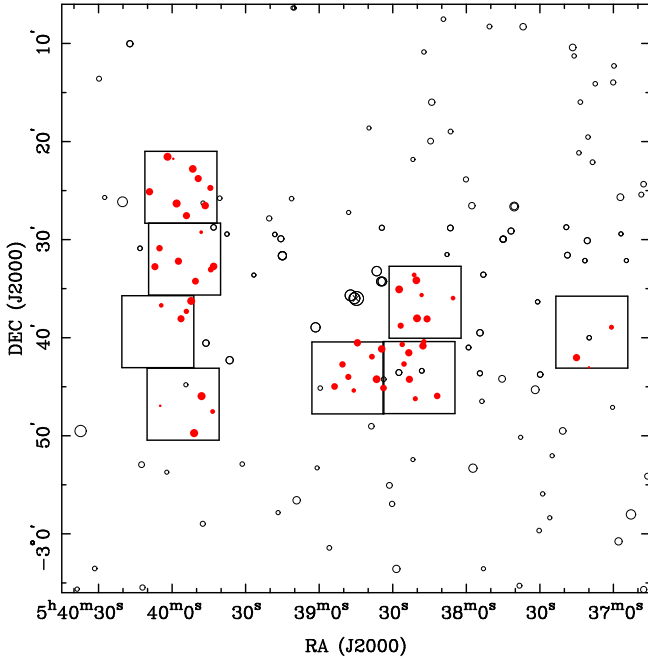


Fig. 1. Location of surveyed fields (open squares) around the star σ Orionis. Our candidates (from Table 2) are indicated by filled circles, while open circles denote field stars brighter than 13 mag. Relative brightness is indicated by symbol size. North is up and East is to the left.

consists of a 1024×1024 Thomson CCD detector, providing a pixel projection of 0.4325 arcsec and a field of view of 7.4×7.4 arcmin² in each exposure. We observed eight different fields in the two filters, covering a total area of 430 arcmin². Exposure times were 1800 s in each filter and field. Table 1 lists the central coordinates of the eight fields. The location of the surveyed region is shown in Figure 1, where some bright stars are indicated. The star σ Orionis, shown at the centre, is also included.

Table 1. Fields coordinates

Field	R.A. (J2000) (h m s)	Dec. (J2000) ($^{\circ}$ ' ")
1	5 38 16.8	-2 36 23
2	5 38 48.3	-2 44 06
3	5 38 19.3	-2 44 04
4	5 39 54.9	-2 31 59
5	5 40 05.8	-2 39 23
6	5 39 56.4	-2 24 40
7	5 39 55.5	-2 46 47
8	5 37 08.8	-2 39 26

Raw frames were reduced within the IRAF¹ environment, using the CCDRED package. Images were bias-subtracted and flatfield-corrected. We combined sky flats

¹ IRAF is distributed by National Optical Astronomy Observatories, which is operated by the Association of Universities for Research in Astronomy, Inc., under contract with the National Science Foundation.

taken at dusk and dawn to obtain the flatfields. The photometric analysis was performed using routines within DAOPHOT, including the selection of objects with a stellar point spread function (PSF) using the DAOFIND task (extended objects were mostly avoided) and aperture and PSF photometry. The nights were photometric, and instrumental magnitudes were transformed into the Cousins RI system using observations of standard stars from Landolt (1992) made every night. Average seeing ranged from 1.5 to 2 arcsec. The survey completeness and limiting magnitudes were $R = 21$, $I = 20$ and $R = 22.5$, $I = 21$, respectively. We adopted as the completeness magnitude the value at which the histogram of detections as a function of magnitude reaches maximum ($\sim 10\text{-}\sigma$ detection); and as limiting magnitude the value at which less than 50% of the objects at the maximum of the histogram are detected ($\sim 3\text{-}\sigma$ detection limit).

We have constructed I vs. $R - I$ colour-magnitude diagrams for each field in order to identify cool cluster members. Figure 2 shows the combination of these diagrams for all the fields. We consider as candidate members objects redder and brighter than the field stars, following the cluster sequence previously defined in BZOR. The lower envelope to the photometric sequence delineated by previously spectroscopically confirmed members is used to separate our candidates from interlopers and background sources. We have selected 53 candidate members, five of which are known from previous surveys (BZOR). Their magnitudes are in the range $I = 14\text{--}20$ mag, which, according to recent theoretical models, correspond to masses in the range $0.35\text{--}0.015 M_{\odot}$ (D'Antona & Mazzitelli 1997; 1998; Burrows et al. 1997; Baraffe et al. 1998; Chabrier et al. 2000). The substellar mass limit at the age and distance of the σ Orionis cluster is located at $I \sim 16$ mag. Table 2 contains the list of selected candidates: around 31 are stellar and 22 substellar. Photometric data and coordinates are also included. Error bars account for the IRAF magnitude error and the uncertainty of the photometric calibration, which is typically $\pm 0.04\text{--}0.06$ mag. Astrometry was carried out using the USNO-SA2.0 catalogue (Monet et al. 1996); we estimate having achieved a precision better than 2 arcsec. Finder charts (3.7×3.7 arcmin²) are provided in Figures A1 and A2.

2.2. Infrared Photometry

We obtained J - and K_s -band point observations of the selected candidates with the 1.52 m Carlos Sánchez Telescope (TCS), at the Teide Observatory, on 1998 September 18, December 17, 1999 January 23, 24 and 2000 January 27. The infrared camera (CAIN) is equipped with an HgCdTe 256×256 detector (Nicmos 3), which, with its wide optics configuration, provides a pixel projection of 1.00 arcsec, covering an area of 4.3×4.3 arcmin² in each exposure. Total exposure times ranged from 60 to 720 s depending on the filter and the expected magnitude of the candidates.

Raw data were processed within the IRAF environment. Each frame consisted of 9–10 exposures obtained using a dithering pattern on the detector. Final images were obtained combining individual images, properly aligned and

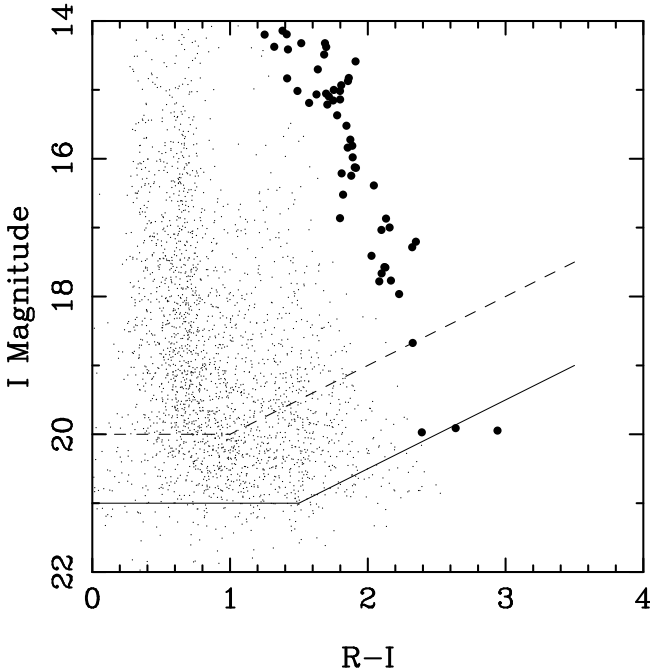


Fig. 2. I vs. $R - I$ colour-magnitude diagram in the σ Orionis cluster resulting from our survey. Filled circles denote our selected candidates listed in Table 2. Completeness and limiting magnitudes are indicated by a dashed and solid line, respectively.

sky-subtracted. Aperture photometry was performed for each object using the PHOT routine within DAOPHOT. A typical radial aperture of 4–5 times the FWHM was adopted. Weather conditions were photometric. Average seeing ranged from 1.6 to 2.2 arcsec. In order to transform instrumental magnitudes into the UKIRT system, each night we observed several field standards (Hunt et al. 1998) and the Pleiades brown dwarf Calar3 (Zapatero Osorio, Martín & Rebolo 1997a).

The photometry of the candidates is shown in Table 2. Error bars include the IRAF magnitude error and the uncertainty of the photometric calibration, which is typically ± 0.05 mag. For 50 of the candidates, all except three, JHK_s photometry is available in the Two Micron All Sky Survey (2MASS) Point Source Catalogue, Third Incremental Release (Cutri et al. 2003). These data are also listed in Table 2. We estimate that the average difference between the 2MASS and TCS photometry in the J band is $J(2MASS) - J(TCS) = 0.012 \pm 0.017$ (where 0.017 stands for the error of the mean, the standard deviation of the differences is 0.116). For the ten candidates for which we have K_s -band photometry in common, the average difference is $K_s(2MASS) - K_s(TCS) = 0.080 \pm 0.040$ (where 0.040 stands for the error of the mean, the standard deviation of the differences is 0.115). For eight of the objects the differences are larger than 0.2 mag in any of the two filters. One is an unresolved binary and other has large error bars in the 2MASS photometry. Small offsets between both data sets could be caused by differences in the filter systems, in the shape and strength of water absorption bands above the observatories, or due to the intrinsic vari-

ability in the atmospheres of some of the targets. In fact, one of the objects with a difference larger than 0.2 mag, S Ori J053825.4-024241, is known to present a strong photometric variability (Caballero et al. 2004). Figure 3 shows the I vs. $I - J$ diagrams for the selected candidates with our photometry (top panel) together with that obtained from the 2MASS catalogue (bottom panel). Figure 4 shows a I vs. $I - K_s$ diagram for those objects with available K_s photometry.

3. Discussion

3.1. Selection of Candidates and Cluster Membership

Colour-magnitude diagrams based on the optical filters R , I and Z have proved to be a good technique for distinguishing true low-mass members from background objects in young nearby clusters (Prosser 1994; Zapatero Osorio et al. 1999; BZOR; Bouvier et al. 1998). We have selected our cluster candidates using optical colour-magnitude diagrams in the R and I bands. The most important sources of contamination in our survey are field M dwarfs. Galaxies are mostly resolved within our completeness magnitude and, given the galactic latitude of the σ Orionis cluster ($b = -17.3$ deg), giant stars are not expected to contribute in a significant number ($< 5\%$) in comparison with main-sequence dwarf stars (Kirkpatrick et al. 1994). According to the density of M field dwarfs obtained by Kirkpatrick et al. (1994), we expect that our proposed photometric sequence for the cluster is not contaminated by field dwarfs of spectral type earlier than M4 and by no more than three of later spectral type within the completeness of our survey. Contamination becomes important in the fainter part of our diagram, where, in addition to the larger error bars, foreground objects can be located in the cluster sequence reddened by the interstellar medium.

To discriminate between bona fide cluster members and field objects, either spectroscopic data or infrared photometry is required. The advantage of the latter is that it can be performed in a shorter integration time in relative small telescopes. The combination of optical and infrared data is a trustworthy technique for distinguishing bona fide cool cluster members (Zapatero Osorio et al. 1997a; Martín et al. 2000; BMZO). The membership of most of the low-mass stars and brown dwarfs ($> 90\%$) identified using both optical and infrared photometric sequences in low-extinction young clusters like the Pleiades have been later confirmed by proper motions, radial velocity or the presence of lithium (Zapatero Osorio et al. 1997b; Moraux, Bouvier & Stauffer 2001). Hence, to confirm that our candidates selected by means of optical diagrams are not reddened field stars, we collected the point near-infrared observations described in Sect. 2.2.

It can be seen from the I vs. $I - J$ colour-magnitude diagrams in Figure 3 that 49 objects show redder colours and magnitudes brighter than the 10 Myr isochrone, which corresponds roughly to the lower envelope of the photometric sequence of previously confirmed members; two candidates with $I \sim 17.5$ and $I - J \sim 1.8$ lie very close to the 10-Myr isochrone in the upper panel of the figure, one of them is the strongly variable object S Ori J053825.4-024241, which

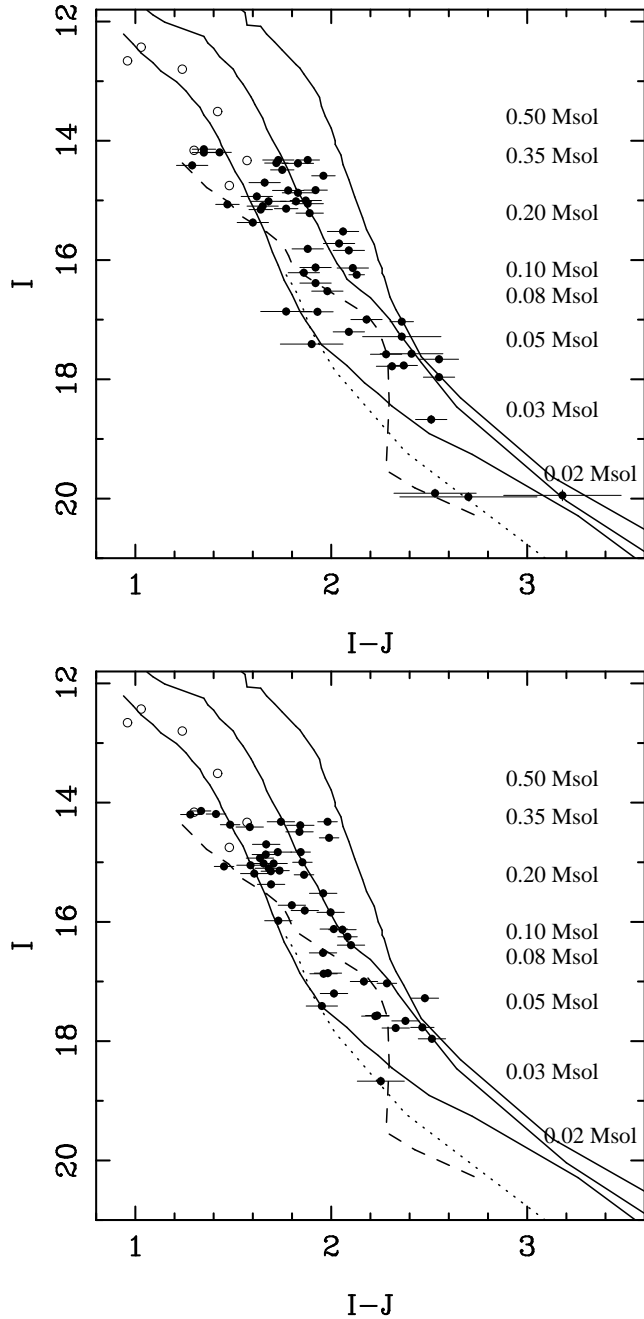


Fig. 3. Top panel: I vs. $I - J$ colour-magnitude diagram of selected candidates in our survey (filled symbols). Open circles denote previously known members taken from Wolk (1996). For comparison, the 1, 3 and 10 Myr Next-Gen theoretical isochrones (solid lines from right to left), from the Lyon group (Baraffe et al. 1998), new 3 Myr dusty isochrones (dotted line) from the Lyon group (Chabrier et al. 2000) and models (dashed line) from D'Antona & Mazzitelli (1998) are also indicated. Bottom panel: I vs. $I - K_s$ colour-magnitude diagram of selected candidates in our survey. As in previous figure, but J -band photometry taken from 2MASS.

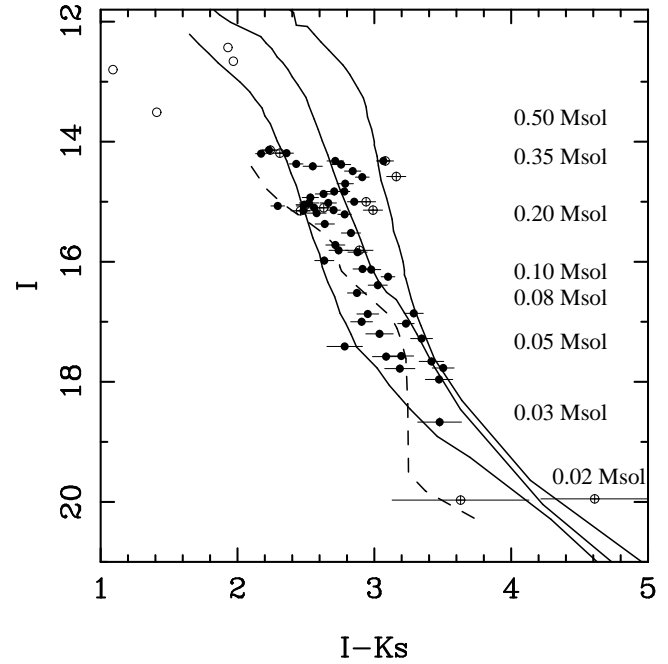


Fig. 4. I vs. $I - K_s$ colour-magnitude diagram of selected candidates. Filled symbols indicate those with 2MASS photometry and open circles with error bars those with TCS photometry. Open circles denote previously known members taken from Wolk (1996). For comparison, the same theoretical isochrones as in the previous figure are plotted.

shows a redder $I - J$ colour according to 2MASS photometry; the other candidate lies on the 10-Myr isochrone when using the 2MASS photometry (bottom panel). All the 51 objects are considered as very likely members. Only two candidates appear to have colours clearly bluer than the 10 Myr isochrone, and are hereafter considered to be probable non-cluster members. There are five candidates in common with the BZOR survey; their cluster membership is supported in both studies. In BZOR we obtained spectroscopy for ten candidates, of which nine were confirmed as cluster members. These nine members follow the infrared photometric sequence of the cluster (BMZO), while the rejected candidate (S Ori 44) has bluer infrared colours. In Table 2 we list spectral types of 13 objects in the present survey. Spectroscopic data have been obtained from Béjar (2000), Zapatero Osorio et al. (2002) and Barrado y Navascués et al. (2003). These spectra show the presence of $H\alpha$ emission in all cases and Li absorption in eight of them observed with higher resolution. As a result, all the objects confirmed by the spectroscopy, have also been previously confirmed by infrared photometry, which argues in favour of the reliability of our selection criteria.

For those objects with available spectroscopy, we have estimated their $R - I$ colour excesses ($E(R - I)$), according to the $R - I$ colour expected for their spectral types, using relations derived by Kirkpatrick & McCarthy (1994), and the $R - I$ photometry obtained here. From Table 2, we can see that all the 13 objects show a visual extinction lower than 1 ($E(R - I) < 0.27$, $A_V < 1$) and all except one show an

extinction lower than 0.25 ($E(R - I) < 0.07$, $A_V < 0.25$). We have obtained K_s photometry for several objects in both surveys. Figure 4 shows the I vs. $I - K_s$ diagram of present paper candidates. These data confirmed our previous results in the J band. In conclusion, although we cannot say, for individual sources, that each candidate belongs to σ Orionis until we have confirmed their cool temperature and youth spectroscopically, or measured their proper motions, we are confident that most of the candidates confirmed with infrared data are bona fide cluster members.

3.2. Near-Infrared Excesses and the Possible Presence of Discs

Using the available JHK_s photometry in the 2MASS catalogue, we have constructed the $H - K_s$ vs. $J - K_s$ colour-colour diagram shown in Figure 5, where we also present Next Gen models (solid lines) from the Lyon group (Baraffe et al. 1998) displaced according to different extinctions, the field dwarf sequence (dashed line) from Bessell & Brett (1988) and Kirkpatrick & McCarthy (1994) and the Classical T Tauri (CTT) star loci (dash-dotted line) from Meyer et al. (1997). Only photometry more accuracy than 0.1 mag. is plotted in Figure 5. From this colour-colour diagram we can see that three out of 48 of our candidates show a near-infrared excess (S Ori J054001.9-022133, S Ori J053943.2-023243 and S Ori J053825.4-024241). The first of these is an M4 low-mass star with an $R - I$ colour of 1.52 ± 0.06 , consistent with its spectral type and with the presence of negligible interstellar extinction (see Table 2). This suggests that the infrared excess is caused by the presence of a disc. For the second, spectroscopy is unavailable and we can not estimate their extinction, so we do not know if the infrared excess is caused by the presence of a disc, interstellar extinction or a local small cloud within the cluster. The last is the strongly variable brown dwarf candidate with an $R - I$ colour of 1.80 ± 0.08 and no available spectroscopy. Its strong infrared excess can not be explained by the existence of normal interstellar reddening and it is most probably related to the presence of a disc. The fraction of objects found with near-infrared excesses is in good agreement with previous studies by Oliveira et al. (2002), who found excesses in only two out of 34 cluster members and Barrado y Navascués et al. (2003), who found excesses in 5–9% of cluster members.

4. Conclusions

In this paper we present an RI survey of the σ Orionis cluster, covering an area of 430 arcmin^2 . We have selected 53 candidates in the magnitude range $14 < I < 20$ that follow the optical photometric sequence of the cluster corresponding to masses in the range $0.35\text{--}0.015 M_\odot$. All but two of the candidates follow the cluster sequence in the infrared and are considered to be likely cluster members: around 31 are stars and 20 are brown dwarfs. The available spectroscopy for some of these objects confirms them as bona fide members. Using near-infrared photometry from 2MASS, we conclude

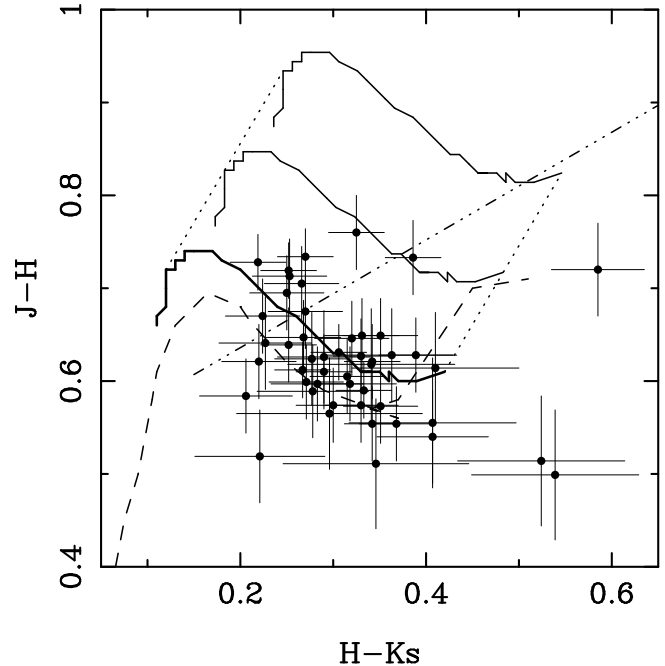


Fig. 5. $J - H$ vs. $H - K_s$ colour-colour diagram of selected candidates with available JHK_s photometry with accuracy better than 0.1 mag. from 2MASS. The 3 Myr Next Gen isochrone from the Lyon group (Baraffe et al. 1998), reddened by visual extinctions of $A_V = 0, 1$ and 2 , are plotted in solid lines from bottom to top. The field dwarf sequence (dashed line) from Bessell & Brett (1988) and Kirkpatrick & McCarthy (1994) and the CTT star loci (dash-dotted line) from Meyer et al. (1997) are also indicated.

that only three of the 48 (6 %) candidates show near-infrared excesses possibly related to the presence of discs.

Acknowledgements. We thank J. Licandro for his help in the acquisition of infrared data at the Carlos Sánchez Telescope and J. A. Caballero and the anonymous referee for their useful comments. We thank I. Baraffe and the Lyon group, F. D’Antona and A. Burrows for sending us electronic versions of their recent models. We are indebted to T. Mahoney for the english revision of this manuscript. This work is based on observations obtained at the TCS and IAC-80 telescope operated by the Instituto de Astrofísica de Canarias at the Spanish Observatorio del Teide (Tenerife, Spain). Partial financial support was provided by the Spanish MCYT project AYA2001-1657. This publication makes use of data products from the Two Micron All Sky Survey, which is a joint project of the University of Massachusetts and the Infrared Processing and Analysis Center/California Institute of Technology, funded by the National Aeronautics and Space Administration and the National Science Foundation. This research has made use of the SIMBAD database, operated at CDS, Strasbourg, France.

References

- Baraffe, I., Chabrier, G., Allard, F., & Hauschildt, P. H. 1998, *A&A*, 337, 403
- Barrado et al. 2003, *A&A*, 404, 171
- Béjar, V. J. S. 2000, PhD. at Universidad de La Laguna.
- Béjar, V. J. S. et al. 2001, *Astrophys. J.*, 556, 830 (BMZO)

- Béjar, V. J. S., Zapatero Osorio, M. R., Rebolo, R. 1999, *Astrophys. J.*, 521, 671 (BZOR)
- Bessell, M. S., & Brett 1988, *PASP*, 100, 1134
- Bouvier, J., Stauffer, J. R., Martín, E. L., Barrado y Navascués, D., Wallace, B., and Béjar, V. J. S. 1998, *A&A*, 336, 490
- Burrows, A., et al. 1997, *Astrophys. J.*, 491, 856.
- Caballero, J. A., Béjar, V. J. S., Rebolo, R., Zapatero Osorio, M. R., 2004, *A&A*, (submitted)
- Chabrier, G., Baraffe, I., Allard, F., & Hauschildt, P. H. 2000, *Astrophys. J.*, 542, 464
- Cutri, R. M. et al. 2003, Explanatory Supplement to the 2MASS Third Incremental Data Release
- D'Antona, F., and Mazzitelli, I. 1997, *MmSAI*, 68, 807
- D'Antona, F., and Mazzitelli, I. 1998, Francesca D'Antona web site at <http://perseus.mporzio.astro.it/~dantona/>
- Haro, M. 1953, *Bol. Obs. Tonantz. Tacub.*, 1, part 7, 11
- Hunt, L. K., Mannucci, F., Testi, L., Migliorini, S., Stanga, R. M., Baffa, C., Lissi, F., Vanzi, L. 1998, *Astron. J.*, 115, 2594
- Kirkpatrick, J. D., & McCarthy, D. W. 1994, *AJ*, 107, 333
- Kirkpatrick, J. D., McGraw, J. T., Hess, T. R., Liebert, J., & McCarthy, D. W. 1994, *ApJS*, 94, 749
- Landolt, A. U. 1992, *AJ*, 104, 340.
- Lee, T. A. 1968, *Astrophys. J.*, 152, 913
- Oliveira, J. M., Jeffries, R. D., Kenyon, M. J., Thomson, S. A., Naylor, T., 2002, *A&A*, 383, L22
- Perryman, M. A. C. et al. 1997, *A&A*, 323, L49
- Martín, E. L., Brandner, W., Bouvier, J., Luhman, K. L., Stauffer, J., Basri, G., and Zapatero Osorio, M. R. 2000, *Astrophys. J.*, 543, 299
- Meyer, M. R., Calvet, N., & Hillenbrand, L. A. 1997, *AJ*, 114, 288
- Monet, D. G., et al. 1996, USNO-SA2.0 (Washington: US Naval Obs.)
- Morau, E.; Bouvier, J.; Stauffer, J. R. 2001, *A&A*, 367, 211
- Prosser, Ch. F. 1994, *Astrophys. J.*, 107, 1422
- Walter, F. M., Wolk, S. J., Freyberg, M., Schmitt, J. H. M. M. 1997, in *Memorie, S. A. It.* 68 N. 4, 1081–1088
- Wiramihardja, S. D., Kogure, T., Yoshida, S., Nakano, M., Ogura, K., & Iwata, T. 1991, *PASJ*, 43, 27
- Wolk, S. J., 1996, Ph. D. University of New York at Stony Brook.
- Wolk, S. J., and Walter, F. M., 1998, in "Very Low-Mass Stars and Brown Dwarfs in Stellar Clusters and Associations" workshop, 11-15 May, La Palma, ed. R. Rebolo & M. R. Zapatero Osorio, in preparation
- Zapatero Osorio, M. R., Béjar, V. J. S., Pavlenko, Ya.; Rebolo, R., Allende Prieto, C., Martín, E. L., García López, R. J. 2002, *A&A*, 384, 937
- Zapatero Osorio, M. R., Martín, E. L., & Rebolo, R. 1997a, *A&A*, 323, 105
- Zapatero Osorio, M. R., Rebolo, R., and Martín, E. L., Basri, G., Magazzù, A., Hodkin, S. T., Jameson, R. F., Cossburn, M. R. 1997b, *ApJ*, 491, L00
- Zapatero Osorio, M. R., Rebolo, R., Magazzù, A., Martín, E. L., Steele, I. A., Jameson, R. F., 1999 *A&AS*, 134, 537

Table 2. Sigma Ori members candidates studied in this paper

Name IAU	Other Name	Finder chart id. num.	I	$R - I$	J	$I - J$	$I - K_s$	2MASS photometry			Sp. Type
								$I - J$	$J - H$	$H - K_s$	
S Ori J053951.1-024944		50	14.14±0.04	1.38±0.06	12.79±0.04	1.35±0.06	2.24±0.06	1.34±0.05	0.67±0.04	0.22±0.04	
S Ori J053958.2-022619 ^a		51	14.19±0.04	1.42±0.06	12.76±0.04	1.43±0.06	2.31±0.06	1.41±0.05	0.73±0.03	0.22±0.03	M3.0
S Ori J053948.1-024557		52	14.20±0.04	1.25±0.06	12.85±0.05	1.35±0.06		1.28±0.05	0.64±0.04	0.25±0.03	
S Ori J054001.9-022133 ^{a,b}		53	14.32±0.04	1.52±0.06	12.44±0.04	1.88±0.06	3.08±0.06	1.98±0.05	0.76±0.04	0.32±0.03	M4.0
S Ori J053952.3-023615		54	14.37±0.04	1.32±0.06	12.65±0.05	1.72±0.06		1.48±0.05	0.70±0.04	0.25±0.04	
S Ori J053820.2-023802 ^{a,c}		55	14.32±0.06	1.69±0.08	12.59±0.05	1.73±0.08		1.74±0.07	0.72±0.03	0.25±0.03	M4.0
S Ori J053836.7-024414		56	14.38±0.06	1.70±0.08	12.55±0.05	1.83±0.08		1.84±0.07	0.65±0.04	0.27±0.04	
S Ori J053827.5-023504 ^{a,d}		57	14.41±0.06	1.42±0.08	13.12±0.05	1.29±0.08		1.58±0.07	0.71±0.04	0.25±0.04	M3.5
S Ori J053820.5-023409 ^{a,c}		58	14.49±0.06	1.68±0.08	12.93±0.05	1.56±0.08		1.84±0.07	0.73±0.03	0.27±0.03	M4.0
S Ori J053951.7-022247 ^a		59	14.59±0.04	1.91±0.06	12.62±0.04	1.97±0.06	3.16±0.07	1.99±0.05	0.59±0.03	0.33±0.03	M5.5
S Ori J053943.2-023243		60	14.70±0.06	1.64±0.08	13.04±0.05	1.66±0.08		1.67±0.07	0.73±0.04	0.39±0.03	
S Ori J053946.6-022631		61	14.83±0.04	1.86±0.06	12.91±0.05	1.92±0.06		1.84±0.05	0.63±0.03	0.30±0.03	
S Ori J053817.8-024050		62	14.87±0.06	1.86±0.08	13.04±0.05	1.83±0.08		1.67±0.07	0.62±0.04	0.34±0.03	
S Ori J054009.3-022507		63	15.00±0.04	1.75±0.06	13.13±0.07	1.87±0.08	2.94±0.04	1.65±0.05	0.65±0.04	0.35±0.04	
S Ori J053823.6-024132		64	14.93±0.06	1.81±0.08	13.31±0.05	1.62±0.08		1.64±0.07	0.55±0.04	0.34±0.03	
S Ori J053715.2-024202 ^a		65	15.07±0.04	1.62±0.06	13.59±0.05	1.48±0.06	2.49±0.03	1.45±0.05	0.62±0.04	0.22±0.04	M4.0
S Ori J053957.5-023212		66	15.02±0.06	1.80±0.08	13.20±0.05	1.82±0.08		1.71±0.07	0.63±0.04	0.33±0.03	
S Ori J053949.4-022346 ^a		67	15.14±0.04	1.80±0.06	13.37±0.04	1.77±0.06	2.99±0.07	1.74±0.05	0.65±0.04	0.32±0.04	M4.0
S Ori J053823.3-024414		68	15.05±0.06	1.70±0.08	13.35±0.05	1.70±0.08		1.59±0.07	0.61±0.04	0.29±0.03	
S Ori J053954.2-022733		69	15.15±0.04	1.75±0.06	13.51±0.04	1.64±0.06	2.46±0.05	1.69±0.05	0.58±0.04	0.21±0.05	
S Ori J054007.1-023245		70	15.10±0.06	1.72±0.08	13.45±0.04	1.65±0.07	2.63±0.08	1.68±0.07	0.61±0.03	0.27±0.03	
S Ori J053956.4-023804		71	15.21±0.04	1.71±0.06	13.32±0.06	1.89±0.07		1.86±0.05	0.55±0.04	0.37±0.04	
S Ori J053950.6-023414		72	15.37±0.06	1.78±0.08	13.77±0.05	1.60±0.08		1.69±0.07	0.67±0.04	0.27±0.04	
S Ori J053845.9-024523		73	15.52±0.06	1.84±0.08	13.46±0.05	2.06±0.08		1.96±0.07	0.60±0.04	0.27±0.04	
S Ori J053811.9-024557		74	15.72±0.06	1.87±0.08	13.68±0.06	2.04±0.08		1.80±0.07	0.63±0.05	0.29±0.05	
S Ori J054005.3-023052 ^a		75	15.81±0.06	1.89±0.08	13.93±0.04	1.88±0.07	2.89±0.10	1.86±0.07	0.57±0.04	0.30±0.04	M5.0
S Ori J053850.6-024244		76	15.84±0.06	1.85±0.08	13.75±0.05	2.09±0.08		2.00±0.07	0.60±0.04	0.28±0.05	
S Ori J053833.9-024508		77	15.98±0.06	1.89±0.07	14.28±0.06	1.70±0.08		1.73±0.07	0.57±0.04	0.33±0.04	
S Ori J053826.8-023846		78	16.12±0.06	1.90±0.08	14.20±0.05	1.92±0.08		2.01±0.07	0.62±0.05	0.28±0.04	
S Ori J053848.1-024401		79	16.13±0.06	1.91±0.08	14.02±0.05	2.11±0.08		2.06±0.07	0.60±0.04	0.31±0.04	
S Ori J053944.4-022445 [*]	S Ori 10	10	16.25±0.04	1.88±0.06	14.12±0.02	2.13±0.04		2.08±0.05	0.63±0.04	0.39±0.04	
S Ori J053944.2-023305 ^{*,e}	S Ori 11	11	16.39±0.06	2.04±0.08	14.47±0.05	1.92±0.08		2.10±0.07	0.57±0.04	0.35±0.04	M6.0
S Ori J053838.6-024157		80	16.52±0.06	1.82±0.08	14.54±0.05	1.98±0.08		1.96±0.07	0.60±0.04	0.31±0.05	
S Ori J053826.2-024041 ^e		81	16.87±0.06	2.13±0.08	14.94±0.06	1.93±0.08		1.96±0.07	0.63±0.05	0.36±0.07	M8.0
S Ori J053954.3-023720		82	17.03±0.04	2.10±0.06	14.67±0.05	2.36±0.06		2.28±0.05	0.54±0.05	0.41±0.06	
S Ori J053817.3-024024 ^{*,a}	S Ori 27	27	17.00±0.06	2.16±0.08	14.82±0.05	2.18±0.08		2.17±0.07	0.52±0.05	0.22±0.07	M6.5
S Ori J053820.8-024613 ^{*,e}	S Ori 31	31	17.20±0.06	2.35±0.08	15.11±0.05	2.09±0.08		2.01±0.07	0.61±0.06	0.41±0.09	M7.0
S Ori J053844.4-024037		83	17.28±0.06	2.32±0.08	14.92±0.20	2.36±0.21		2.48±0.07	0.59±0.05	0.28±0.06	
S Ori J053943.5-024731 [*]	S Ori 32	32	17.57±0.04	2.12±0.06	15.16±0.15	2.41±0.16		2.23±0.06	0.55±0.07	0.41±0.09	
S Ori J053700.9-023856		84	17.41±0.04	2.03±0.06	15.51±0.15	1.90±0.15		1.95±0.08	0.54±0.11	0.29±0.15	
S Ori J053821.3-023336 ^{**}		85	17.58±0.06	2.13±0.08	15.40±0.07	2.18±0.09		2.22±0.07	0.56±0.06	0.30±0.10	
S Ori J053805.5-023557		86	17.66±0.06	2.10±0.11	15.11±0.08	2.55±0.10		2.38±0.07	0.51±0.07	0.52±0.09	
S Ori J054004.5-023642		87	17.77±0.04	2.16±0.06	15.40±0.06	2.37±0.07		2.46±0.06	0.50±0.07	0.54±0.09	
S Ori J053853.8-024459		88	17.78±0.06	2.08±0.08	15.47±0.05	2.31±0.08		2.33±0.07	0.51±0.07	0.35±0.10	
S Ori J053818.2-023539		89	17.96±0.06	2.23±0.08	15.41±0.05	2.55±0.08		2.51±0.07	0.62±0.06	0.34±0.09	
S Ori J053948.1-022914 ^{**,e}		90	18.67±0.07	2.33±0.10	16.16±0.03	2.51±0.08		2.25±0.12	0.83±0.13	0.40±0.17	M7.0
S Ori J053710.0-024302 ^f		92	19.95±0.09	2.94±0.33	16.77±0.30	3.18±0.30	4.6±0.4				M8.0
S Ori J053834.5-024109		94	14.83±0.06	1.41±0.08	13.05±0.05	1.78±0.08		1.73±0.07	0.65±0.04	0.33±0.04	
S Ori J053844.4-024030		95	15.02±0.06	1.49±0.08	13.34±0.07	1.68±0.09		1.65±0.07	0.64±0.05	0.23±0.05	
S Ori J053816.0-023805		96	15.19±0.06	1.57±0.08				1.61±0.07	0.70±0.04	0.27±0.04	
S Ori J053825.4-024241		97	16.86±0.06	1.80±0.08	15.09±0.11	1.77±0.13		1.98±0.07	0.72±0.05	0.58±0.05	
				Probably	non	members					
S Ori J054004.9-024656		91	19.91±0.07	2.64±0.28	17.38±0.20	2.53±0.20					
S Ori J053959.5-022146		93	19.97±0.07	2.39±0.25	17.27±0.35	2.70±0.35	3.6±0.5				

* IAU name from BZOR

** IAU name from BMZO

a. Spectroscopic data from Zapatero Osorio et al. 2002. All these objects have Li.

b. Haro 5-36, from Haro, M. 1953

c. X-ray source from Wolk 1996

d. Kiso A-0976 329 from Wiramihardja et al. 1991

e. Spectroscopic data from Barrado y Navascués et al. 2003

f. Spectroscopic data from Béjar 2000

Appendix A: Finder charts.

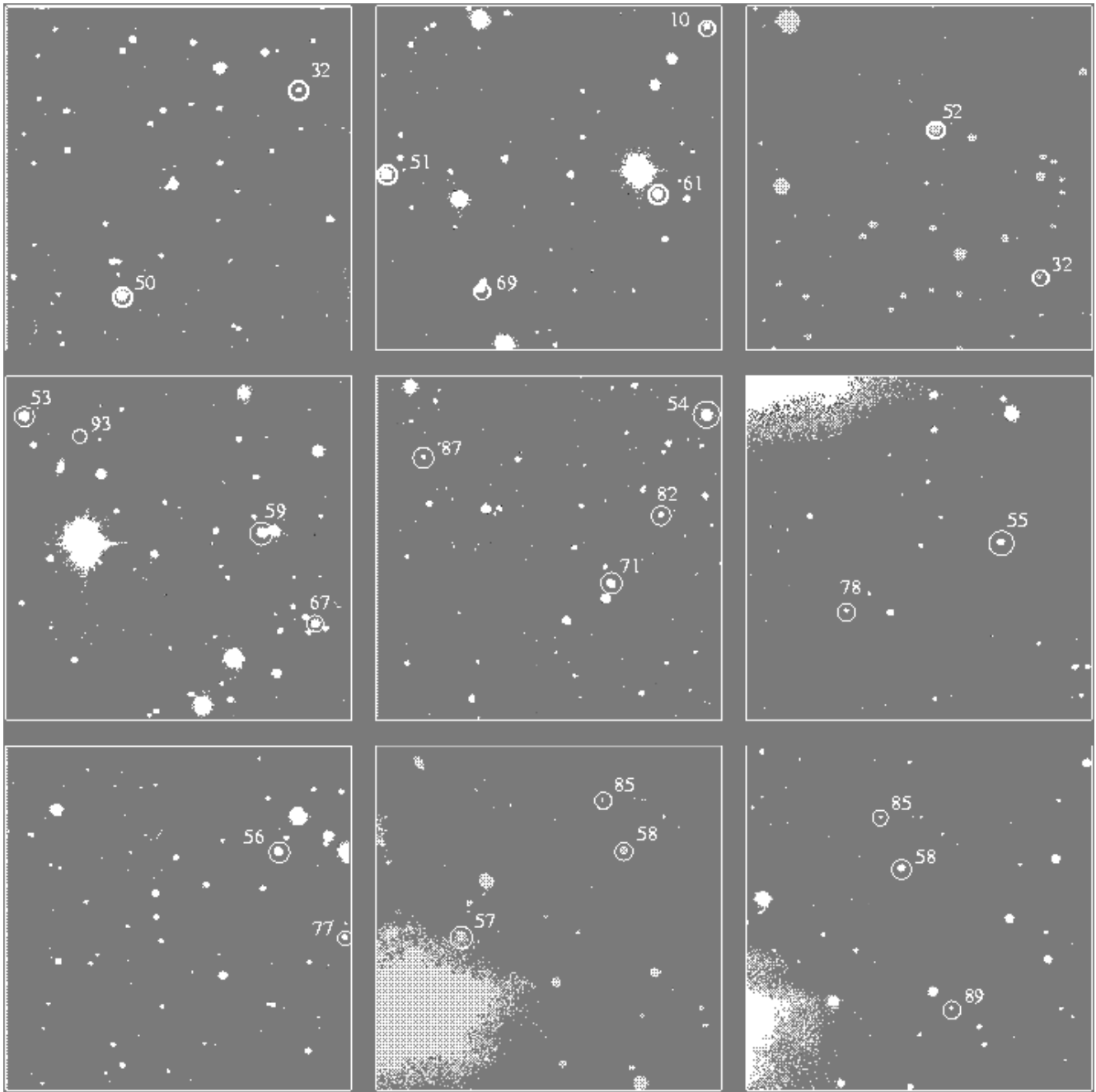


Fig. A1. Finder charts in the *I*-band ($3.7' \times 3.7'$). North is up and East is left.

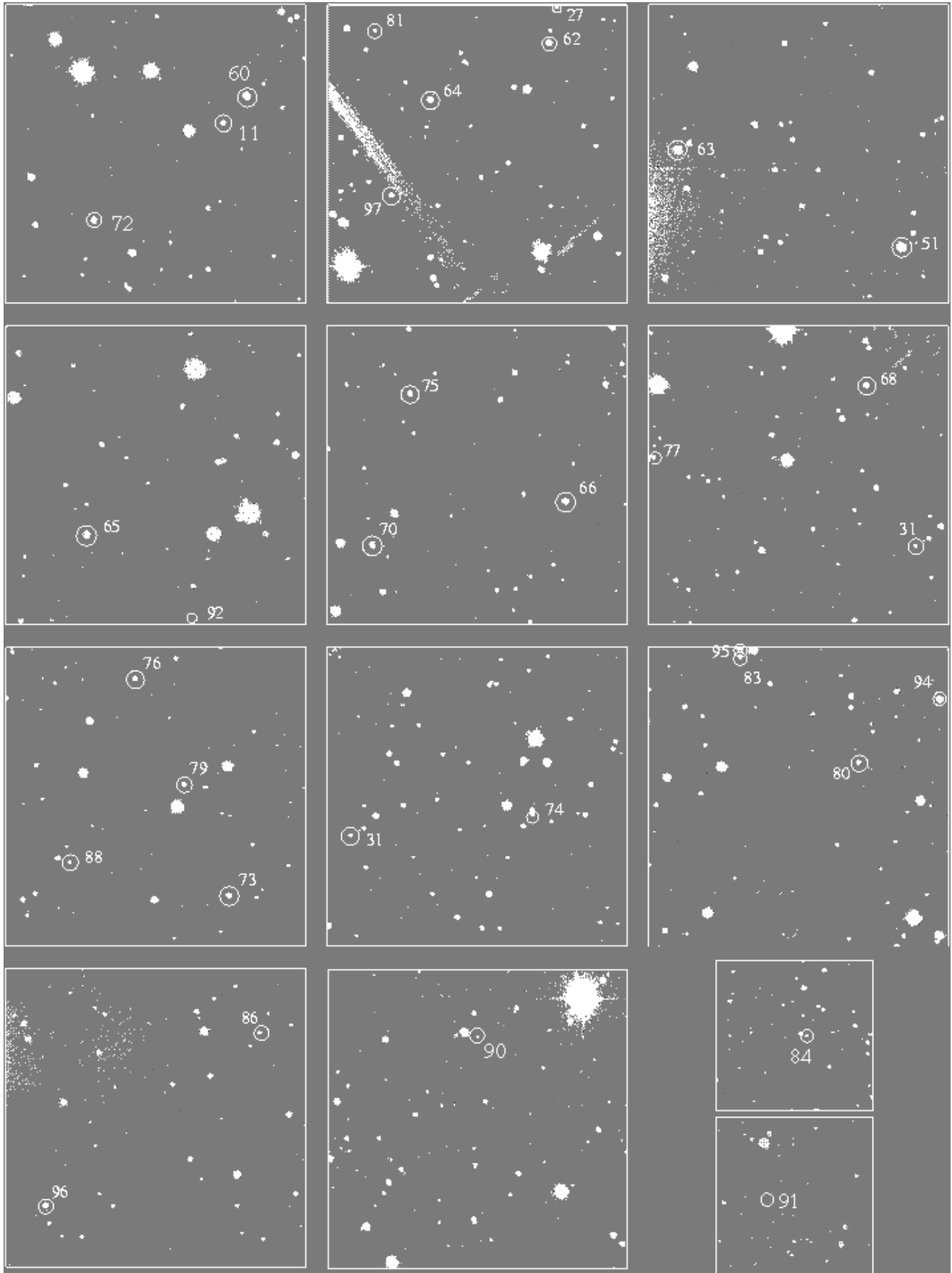


Fig. A2. Finder charts in the *I*-band ($3.7' \times 3.7'$). North is up and East is left (continuation).